The G Protein–Activating Peptide, Mastoparan, and the Synthetic NH_2-terminal ARF Peptide, ARFp13, Inhibit In Vitro Golgi Transport by Irreversibly Damaging Membranes

Peggy J. Weidman and William M. Winter

Department of Biochemistry and Molecular Biology, St. Louis University Medical School, St. Louis, Missouri 63104

Abstract. Mastoparan is a cationic amphipathetic peptide that activates trimeric G proteins, and increases binding of the coat protein β-COP to Golgi membranes. ARFp13 is a cationic amphipathic peptide that is a putative specific inhibitor of ARF function, and inhibits coat protein binding to Golgi membranes. Using a combination of high resolution, three-dimensional electron microscopy and cell-free Golgi transport assays, we show that both of these peptides inhibit in vitro Golgi transport, not by interfering in the normal functioning of GTP-binding proteins, but by damaging membranes. Inhibition of transport is correlated with inhibition of nucleotide sugar uptake and protein glycoslation, a decrease in the fraction of Golgi cisternae exhibiting normal morphology, and a decrease in the density of Golgi-coated buds and vesicles. At peptide concentrations near the IC_{50} for transport, those cisternae with apparently normal morphology had a higher steady state level of coated buds and vesicles. Kinetic analysis suggests that this increase in density was due to a decrease in the rate of vesicle fission. Pertussis toxin treatment of the membranes appeared to increase the rate of vesicle formation, but did not prevent the membrane damage induced by mastoparan. We conclude that ARFp13 is not a specific inhibitor of ARF function, as originally proposed, and that surface active peptides, such as mastoparan, have the potential for introducing artifacts that complicate the analysis of trimeric G protein involvement in regulation of Golgi vesicle dynamics.

THE movement of secretory proteins through the Golgi complex may involve multiple vesicular transport steps. Genetic and biochemical studies have revealed that the trafficking of transport vesicles is regulated by members of at least three different GTP-binding protein families: Rab proteins (37), ADP-ribosylation factors (ARFs;[1] 35), and trimeric G proteins, (4, 7). The molecular details of these regulatory pathways, however, have been difficult to elucidate.

Peptides designed to interfere with GTP-binding protein activity have been widely used as probes for the function of GTP-binding proteins in protein transport. These include peptides corresponding to the putative effector domain of Rab proteins (16, 30, 39, 40), peptides that correspond to the NH_2-terminal domain of ARF proteins (3, 24, 28, 34), and peptides that mimic the trimeric G protein interacting domain of G protein–coupled receptors (9, 10, 13, 26, 29). A role for these various GTP-binding proteins in protein transport, as suggested by peptide studies, has in many cases been substantiated by independent approaches (15, 48, 49, 54). Nevertheless, the characteristics of peptide action in in vitro transport systems are often different than those observed when the cognate GTP-binding protein is inactivated by other means (15, 49) or removed (47). Moreover, competition between peptides and their cognate GTP-binding proteins has been difficult to demonstrate (24, 47), raising the possibility that some peptide reagents are not as specific as originally thought (31).

We have used the in vitro Golgi transport system of Rothman and colleagues to investigate the mechanism of action of two peptides reported to have opposing effects on coat protein binding to Golgi membranes. Mastoparan (MAS; Fig. 1 *A*), is a cationic amphipathic peptide that stimulates trimeric G protein GTP/GDP exchange by mimicking the interaction domain of G protein–coupled receptors (21, 22). In semi-intact cells, this peptide stimulates binding of the vesicle coat protein, β-COP, to Golgi membranes (26). The stimulatory effect of the peptide is largely abolished by pertussis toxin-catalyzed ADP ribosylation of $G_{\alpha i/o}$ subunits. These findings are consistent with other evidence that tri-

Address all correspondence to P. J. Weidman, Department of Biochemistry and Molecular Biology, St. Louis University Medical School, 1402 S. Grand Blvd., St. Louis, MO 63104. Ph.: (314) 577-8179. Fax: (314) 577-8156.

Abbreviations used in this paper: ARF, ADP-ribosylation factor; BFA, brefeldin A; COP, coat proteins; Gal, galactose; GlNAc, *N*-acetylglucosamine; LCRI, low cytosol-requiring intermediate; MAS, mastoparan; NSF, NEM-sensitive factor; VSV, vesicular stomatitis virus; VSV-g, VSV glycoprotein.

meric G proteins regulate vesicle coat protein binding to the Golgi complex (17, 33, 41, 45). ARFp13 is an amphipathic peptide corresponding to the NH_2-terminal sequence of ARF (Fig. 1 *B*), which is thought to be a critical determinant of ARF activities (24). This peptide is a potent inhibitor of the ADP-ribosylating activity of ARF (24), of transport in several in vitro systems (3, 24, 28), and of vesicle formation on Golgi membranes (24). Although this peptide has been proposed to compete with ARF, competition has not been demonstrable (24, 47). Given the structural similarity between these NH_2-terminal sequences of ARF and MAS, it has been suggested that ARF may interact with a trimeric G protein to exert its effects (24). The ability of MAS to stimulate and ARFp13 to inhibit coat protein binding could thus represent activation of different trimeric G proteins that have opposing roles in the regulation of vesicular transport, as has been proposed for vesicle formation in the TGN (4).

We demonstrate that both MAS and ARFp13 are potent inhibitors of in vitro Golgi transport. Inhibition is specific for MAS analogs that stimulate nucleotide exchange on purified G protein subunits, and for ARF peptides that inhibit the ADP-ribosylating activity of ARF. Nevertheless, inhibition is not due to activation of G proteins, but rather to a generalized effect on membrane function, including inhibition of nucleotide sugar uptake and protein glycosylation. Morphological analysis using high resolution, three-dimensional imaging reveals that these amphipathic peptides induce changes in cisternal architecture indicative of membrane damage. The significance of these findings and their implications are discussed.

Materials and Methods

Materials and Reagents

Golgi-enriched membranes were prepared as previously described (1). Donor Golgi were prepared from *N*-acetylglucosamine (GlcNAc) transferase I-deficient CHO Lec 1 cells (44) infected with vesicular stomatitis virus (VSV) in suspension culture (12). Acceptor Golgi were prepared from CHO Pro^{-5} cells (parental line of CHO Lec 1; 44). CHO cytosol was prepared from CHO Lec 1 cells as described by Block et al. (5). Bovine brain cytosol fractions 1,2,3, and 4 were prepared according to the procedure of Clary and Rothman (11). ARF-depleted cytosol was prepared as described by Taylor and Melançon (46). UDP-[^{3}H]-*N*-GlcNAc was synthesized from [^{3}H]-glucosamine (New England Nuclear, Wilmington, DE) using the method of Lang and Kornfeld (27). Protein concentrations were determined with bicinchoninic acid (43; Pierce, Rockford, IL). MAS was purchased from Sigma Chemical Company (St. Louis, MO). MAS 7 and MAS 17 were kind gifts of Drs. M. Colombo and P. Stahl (Washington University, St. Louis, MO). ARFp13 and ARFp28 were kind gifts of Drs. J. Donaldson and R. Klausner (National Institutes of Health, Bethesda, MD). To facilitate direct comparisons, the peptide concentrations were determined by ninhydrin assay after alkaline hydrolysis (23) using leucine as standard. All of the peptide preparations were found to contain significant amounts of non-peptide solids (50–80%). All reagents were of the highest grade available.

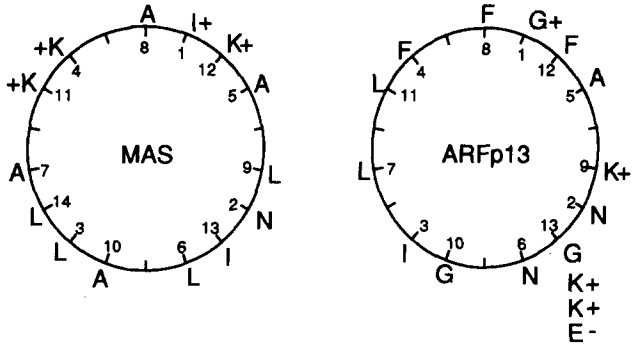

Figure 1. Helical wheel projections of MAS and ARFp13. (*A*) Helical wheel projection of MAS. The active analog, MAS7, has A and L at positions 12 and 13, respectively. The inactive analog, MAS17, has K and L at positions 6 and 13, respectively. (*B*) Helical wheel projection of the first 13 amino acids of ARFp13, as described by Kahn et al. (24). The inactive analog, ARFp28, is lacking the first four amino acids of the sequence.

Cell-free Golgi Transport Assays

Golgi transport assays were performed as previously described (1). A typical 25 μl Golgi transport assay contained 2.5 μl each of donor and acceptor membranes, 2.5 μl of cytosol, 10 μM palmitoyl coenzyme A, an ATP-regenerating system (50 μM ATP, 5 mM creatine phosphate, 11.9 IU/ml creatine phosphokinase), 250 μM UTP, 0.1 mM DTT, 0.2 M sucrose, 0.25 μCi UDP-[^{3}H]-GlcNAc, and buffer salts (25 mM Hepes, pH 7.0, 20 mM KCl, 2.5 mM magnesium acetate). The concentrations of membrane and cytosolic protein are stated in the figure legends. Assays were incubated for 60 min at 37°C, and VSV glycoprotein (VSV-g) protein was immunoprecipitated and collected on filters for scintillation counting.

Assays for Glycosylation, Nucleotide Sugar Uptake, and Membrane Integrity

A two stage incubation was used to measure inhibition of glycosylation after VSV-g protein had been transported to the acceptor compartment (20). In stage I, a standard Golgi transport assay mixture lacking UDP-[^{3}H]-GlcNAc was incubated for 45 min at 37°C to allow VSV-g protein to accumulate in the acceptor compartment. Inhibitors were then added, and the incubation continued for an additional 15 min at 37°C. In stage II, the Golgi membranes were re-isolated by centrifugation, and then incubated at 37°C in 25 μl of glycosylation buffer (25 mM Hepes, pH 7.0, 15 mM KCl, 2.5 mM Mg acetate, 0.2 M sucrose, ATP-regenerating system, 250 μM UTP, 250 μg/ml nucleotide monophosphate kinase, and 0.25 μCi UDP-[^{3}H]-GlcNAc; 20) for up to 80 min, followed by immunoprecipitation of VSV-g protein, as described above.

Soluble assays for galactose (Gal) and GlcNAc transferase activities were performed as described by Dunphy and Rothman (18). Glycosylation of VSV-g protein and nucleotide sugar uptake were measured with VSV-infected Pro^{-5} (wild type) membranes that were rendered incompetent for transport by inactivation of the NEM-sensitive factor (NSF) (5, 35). The membranes were incubated in a standard transport reaction mixture containing 0.25 μCi of either UDP-[^{3}H]-GlcNAc, UDP-[^{3}H]-Gal, or CMP-[^{3}H]-sialic acid plus 10 μM CTP, with or without inhibitors. Nucleotide sugar uptake was measured after 15 min of incubation by removing duplicate 25 μl samples, diluting them with 75 μl of cold buffer (25 mM Hepes, pH 7.0, 15 mM KCl, 2.5 mM Mg acetate, 0.3 M sucrose), and isolating the membranes by centrifugation in a microfuge for 5 min. The pellets were washed twice with 100 μl of cold buffer, and transferred to vials for scintillation counting. Glycosylation of endogenous VSV-g protein was measured by immunoprecipitating VSV-g protein from duplicate 25 μl samples of the reaction mixture after a 1-h incubation (47).

Membrane integrity was assessed by incubating VSV-infected Pro^{-5} membranes in a transport reaction for 5 min to accumulate UDP-[^{3}H]-GlcNAc in Golgi compartments, thereby establishing a concentration gradient of UDP-[^{3}H]-GlcNAc across the membrane (50). The membranes were then incubated for an additional 10 min with inhibitors to determine whether the nucleotide sugar gradient was maintained. Duplicate 25 μl samples were centrifuged and the total amount of [^{3}H] in the membrane pellets was determined as described above. To correct for [^{3}H] incorporated into protein during the incubation, duplicate 25 μl samples were centrifuged, the pellets solubilized in 25 μl of 0.015% sodium deoxycholate, and the protein precipitated with 5% cold TCA. The precipitate was collected by centrifugation, washed twice with 100 μl of cold ethanol, and transferred to vials for scintillation counting. The soluble UDP-[^{3}H]-GlcNAc remaining in the membranes was determined by subtracting the radioactivity incorporated into protein from the total radioactivity of the pellets.

The effect of the peptides on the sedimentation of Golgi membranes was

examined by first labeling Golgi proteins in VSV-infected Pro^{-5} membranes by incubation in a transport reaction mixture for one hour. Inhibitors were added and the mixtures incubated an additional 10 min at 37°C. Duplicate 25 μl samples were centrifuged and the radioactive protein in the pellet determined by TCA precipitation, as described above.

Preparation of Pertussis Toxin-treated Membranes

CHO lec 1 and Pro^{-5} cells were incubated for three hours in media containing 0.1 μg/ml pertussis toxin along with parallel cultures of untreated cells. After this treatment, the lec 1 cells were infected with VSV following the standard protocol, and donor and acceptor membrane fractions were then prepared from homogenates of treated and untreated cells. The extent of ADP ribosylation of G_α subunits in vivo was determined by in vitro ADP ribosylation of treated and untreated membranes with [^{32}PI]-NAD and pertussis toxin (6). The relative content of [^{32}P] in the samples was determined by densitometry after SDS-PAGE and autofluorography. Approximately 80% of G_α was ADP ribosylated in vivo in both the donor and acceptor membrane fractions. The amount of [^{3}H]-GlcNAc incorporated into VSV-g protein in assays containing 1 μg each of donor and acceptor membrane was 2,400 cpm for mock-treated membranes, and 2,500 cpm for pertussis toxin-treated membranes. A second preparation of membranes gave qualitatively similar results.

Electron Microscopy

Freshly isolated Golgi-enriched membrane fractions were immobilized on 3 mm^2 polylysine- and glutaraldehyde-treated coverslips, as previously described (53). The amount of membrane protein immobilized per coverslip was 0.08 ± 0.02 μg, as determined with ^{35}S-labeled membranes. The immobilized membranes were incubated in vitro with 8 μl of a standard transport reaction mixture (0.01 μg/ml membrane protein) for 10 min. Since the effects of the inhibitors under study were strongly dependent on both the cytosol and membrane protein concentrations, titrations of the inhibitors in 100 μl, standard transport reactions containing 0.01 μg/ml total membrane protein were used to determine the relevant concentration ranges for cytosolic protein and inhibitors used in these studies, as stated in the legends. After in vitro incubation, the immobilized membranes were fixed, quick frozen, deep-etched, and replicas prepared for transmission electron microscopy, as previously described (19, 53).

Quantitative Analysis of Electron Micrographs

Micrographs of Golgi membranes were taken from two coverslips for each experimental sample (approximately 10 micrographs per coverslip). 100–150 negatives from each experiment containing six to eight individual samples, were randomized for analysis. Negatives were projected at 2.6-fold magnification onto a 15 or 20 mm^2 grid using a Bessler enlarger. The negative number, the magnification, the number of coated buds and vesicles, the area encompassing the Golgi membranes relative to the grid, and abnormal morphological characteristics, such as the presence of long tubules, clusters of uncoated bud-like protrusions, irregular fragments of tubules and vesicles, were recorded. After all of the negatives for a given experiment were scored, the data were entered into a spreadsheet program, sorted by negative number, and then grouped by experimental sample for calculation of the average bud and vesicle densities and the fraction of complexes exhibiting abnormal morphology.

Results

Inhibition of Transport Is Specific for Active Peptides

The in vitro Golgi transport assay was used to biochemically characterize the inhibition of transport caused by MAS and ARFp13. As shown in Fig. 2 *A*, MAS is the more potent peptide inhibitor with an IC_{50} of 0.75 μM. MAS 7, a variant of MAS that also stimulates GDP/GTP exchange on trimeric G proteins (22), is equally effective at inhibiting transport. In contrast, an inactive variant of MAS, MAS17 (22), is not inhibitory, indicating that inhibition is specific for peptides that activate trimeric G proteins. The concentrations of MAS and MAS7 that inhibit transport are similar to those that inhibit release of vesicles from the TGN in vitro (29), but lower than those that induce binding of β-COP to isolated Golgi membranes and Golgi membranes in semi-intact cells (26). The NH_2-terminal ARF peptide, ARFp13, a potent inhibitor of ARF ADP-ribosylating activity (24), inhibits transport with an IC_{50} of 20–25 μM (Fig. 2 *B*), as previously reported by others (24). ARFp28, a shorter peptide that has no effect on the ADP-ribosylating activity of ARF, is not inhibitory, indicating that inhibition of transport is correlated with ability to block other ARF-dependent functions. The inhibition of transport caused by both peptides thus meets these basic criteria for specificity.

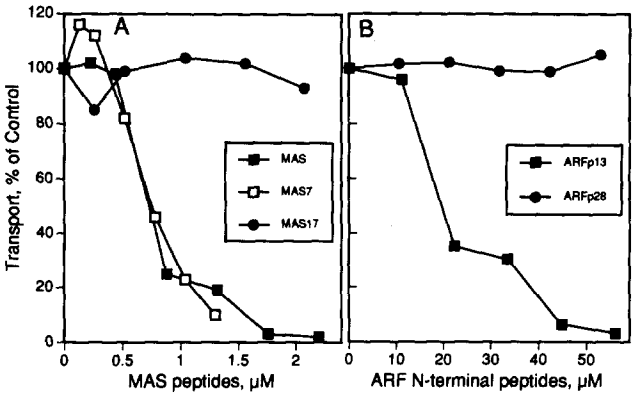

Figure 2. MAS and ARF peptides exhibit the selectivity expected for specific inhibitors of in vitro Golgi transport. Standard in vitro Golgi transport assays were performed as described in Materials and Methods. (*A*) Incubations contained 0.3 and 0.15 mg/ml cytosolic and membrane protein, respectively, and the indicated concentration of MAS (■), MAS7 (□), or MAS 17 (●). In the absence of peptide, the incorporation of [^{3}H]-GlcNAc into VSV-g protein was 3,4000 cpm (n = 3). (*B*) Incubations contained 0.35 and 0.14 mg/ml cytosolic and membrane protein, respectively, and the indicated concentration of ARFp13 (■) or ARFp28 (●). In the absence of peptide, the incorporation of [^{3}H]-GlcNAc into VSV-g protein was 8,300 cpm. The biochemical data shown in this and all other figures and tables are representative of two or more independent experiments.

Inhibition Is Sensitive to Membrane and Cytosolic Protein Concentrations

It has been shown that activation of reconstituted trimeric G proteins by MAS is dependent on the ratio of MAS to phospholipid (21), and not on the total concentration of MAS in solution. This suggests that it is the concentration of peptide in the membrane, not the total concentration, that determines the extent of response (21). For both MAS and ARFp13, the effective peptide concentration for inhibition of transport increases with increasing concentration of Golgi-enriched membranes in the assay (Table I *A*). This is consistent with a membrane-associated mode of action for both MAS and ARFp13.

The IC_{50} for both peptides also increased with increasing concentration of cystosol in the transport assay (Table I *B*). The ability of cytosol to abrogate ARFp13-induced inhibition is not due to competition with cytosolic ARF. It has previously been shown that inhibition by ARFp13 is independent of the ARF concentration in the assay (47). We also found that the IC_{50} for MAS and ARFp13 was the same

Table I. Peptide Inhibition Is Sensitive to the Cytosolic and Membrane Protein Concentrations

	MAS	ARFp13
	IC_{50} (μM)	
(*A*) Membrane concentration		
0.11 mg/ml	1.7	32
0.22 mg/ml	2.3	37
0.44 mg/ml	3.0	41
(*B*) Cytosol concentration		
0.14 mg/ml	0.6	10
0.28 mg/ml	0.8	18
0.56 mg/ml	1.2	28

The concentration of MAS and ARFp13 that produced half maximal inhibition of the in vitro Golgi transport assay (IC_{50}) were determined from the best polynomial fit of titration curves, such as those in Fig. 1. (*A*) Each titration contained the indicated concentration of membrane protein and 0.58 mg/ml cytosol. (*B*) Each titration contained the indicated concentration of cytosol and 0.10 mg/ml membrane protein.

when assayed with either normal or ARF-depleted (46) cytosol (data not shown). Four fractions of bovine brain cytosol that together contain all of the necessary soluble factors for transport (11) were tested individually for their ability to block the inhibition. All four fractions were equipotent in their ability to shift the IC_{50} of each peptide (data not shown), suggesting that there is no single component responsible for the blocking activity of cytosol. Preincubation of the peptides with cytosol at 37°C resulted in loss of their inhibitory activity over a period of 5–15 min, suggesting that the peptides were being degraded or otherwise inactivated. This loss of inhibitory activity was not prevented by protease inhibitors such as phenymethylsulfonyl fluoride, leupeptin, peptstatin, or aprotinin, but was significantly slowed by treating the cytosol with 1 mM NEM at 37°C for 15 min before adding the peptide (data not shown). The blocking effect of cytosol thus appears to result from accelerated inactivation of the peptides, and not competition between a specific cytosolic factor and the peptides.

MAS and ARFp13 Inhibit the Same Late Step in Intra-Golgi Transport

The observation that MAS stimulates (26) and ARFp13 inhibits (24) β-COP binding to Golgi membranes suggests that these peptides should block transport at different stages. To delineate the last step in transport that is sensitive to each peptide, the rates of formation of transport intermediates that are resistant to inhibition by these peptides was determined (2). In this analysis, inhibitor is added at various times after initiation of the transport incubation. The incubation is then continued to permit existing transport intermediates that are resistant to the inhibitor to complete the transport cycle. Fig. 3 *A* show the rates of formation of previously characterized transport intermediates. The low cytosol requiring intermediate (LCRI; 51) is formed very early in the reaction, and the GTPγS-resistant intermediate (GTPγS; 33) forms somewhat later. The 37°C NEM-resistant intermediate (NEM; 2) is formed only very late in the reaction, as indicated by the overall rate of VSV-g protein transport and glycosylation in the absence of inhibitors (ice). Under these conditions, NEM inactivates not only NSF but other components as well (52; see below).

Fig. 3 (*B* and *C*) shows that intermediates resistant to

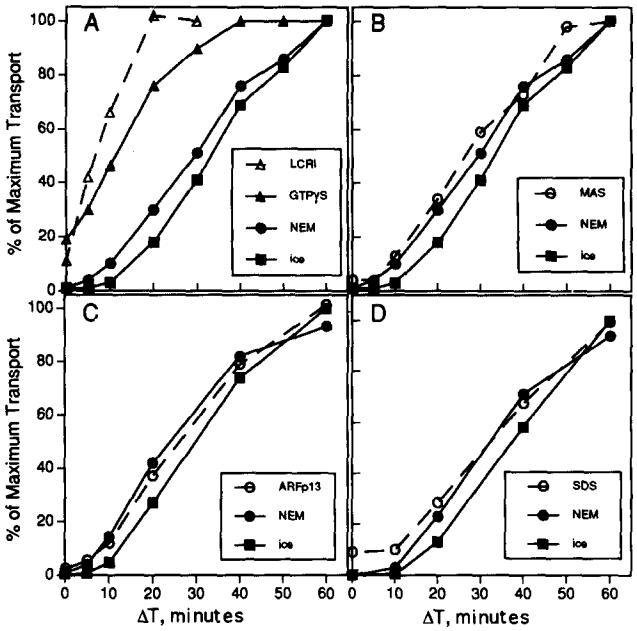

Figure 3. Transport becomes resistant to inhibition by MAS and ARFp13 only very late in the transport reaction. In vitro transport was initiated by transferring reaction mixtures to 37°C. At the indicated times (ΔT), inhibitors were added and the incubation continued for a total of 60 min to permit inhibitor-resistant transport intermediates to complete the transport process. (*A*) The rate of formation of previously characterized transport intermediates: the LCRI (Δ) was detected by diluting the transport reaction fivefold with a reaction mixture lacking cytosol; the GTPγS resistant intermediate (▲) was detected by adding 10 μM GTPγS; and 1 mM NEM was added to detect the 37°C NEM-resistant intermediate (●). For comparison, the rate of VSV-g protein transport in the absence of inhibitors was monitored by terminating the reaction on ice (■). The maximum incorporation of [^{3}H]-GlcNAc into VSV-g protein at 60 min for all samples was 4,600 cpm. (*B–D*) The rate of formation of the 37°C NEM-resistant intermediate (●) and the overall rate of VSV-g protein transport (■) is compared with the rates of formation of transport intermediates resistant to (*B*) 2.2 μM MAS, (*C*) 56 μM ARFp13, and (*D*) 50 μM SDS (○). The maximum incorporation of [^{3}H]-GlcNAc into VSV-g protein for all samples at 60 min was 4,500 (*B*), 19,500 (*C*), and 8,200 cpm (*D*).

MAS and ARFp13, respectively, form only very late in the transport reaction, coincident with the formation of the NEM-resistant intermediate. Thus, in contrast to the prediction, both peptides block the same step in transport, and this block occurs very late in the reaction, when transport is nearly complete. Moreover, inhibition of the same late transport step is also observed with low concentrations of the anionic detergent, SDS (Fig. 3 *D*). Inhibition of this late transport step is thus not specific for cationic amphipathic peptides, as expected if inhibition was due to activation of a trimeric G protein.

MAS and ARFp13 Inhibit Glycosylation of VSV-g Protein

It has been demonstrated that glycosylation becomes the rate determining step in the measurement of VSV-g protein transport in this assay (20, 47). The late transport step inhibited by these peptides might thus correspond to inhibition of

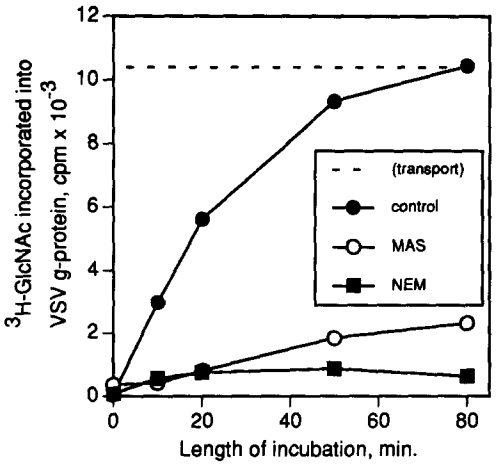

Figure 4. MAS inhibits glycosylation of VSV-g protein after its delivery to the acceptor compartment. Membranes were incubated in a standard transport reaction lacking UDP-[^{3}H]-GlcNAc for 45 min to accumulate VSV-g protein in the acceptor compartment. The reaction mixture was split into three parts and incubated at 37°C for an additional 15 min with either no inhibitor (●), 2.2 μM MAS (○), or 1 mM NEM (■). After neutralization of unreacted NEM with 2 mM DTT, the membranes were re-isolated by centrifugation and incubated in a glycosylation buffer containing UDP-[^{3}H]-GlcNAc for the indicated times (see Materials and Methods for details). The dashed line indicates the amount of incorporation observed in a control sample where UDP-[^{3}H]-GlcNAc was added at the beginning of the transport incubation.

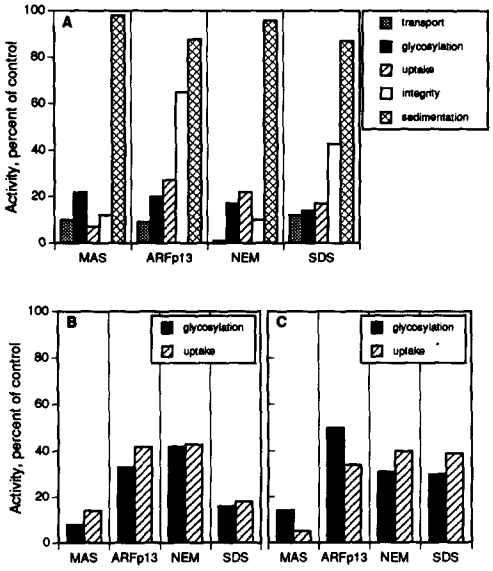

Figure 5. Late inhibition of transport correlates with generalized inhibition of nucleotide sugar uptake and protein glycosylation. MAS (3.3 μM), ARFp13 (43 μM), NEM (1 mM), or SDS (50 μM) were added to standard transport reaction mixtures containing 0.3 mg/ml cytosolic protein and 0.15 mg/ml of either donor and acceptor membranes (transport) or transport incompetent, VSV-infected wild type membranes (all other measurements). The effects of the inhibitors on glycosylation of endogenous VSV-g protein, uptake of nucleotide sugars, membrane integrity as measured by retention of UDP-[^{3}H]-GlcNAc, and sedimentation of [^{3}H]-GlcNAc-labeled proteins with Golgi membranes were measured as described in Materials and Methods. The values for each inhibitor are expressed as percent of the control (no inhibitor) and are the average of duplicate determinations. The deviation of duplicates from the average in all samples was 7% or less. (*A*) Reaction mixtures contained 0.25 μCi UDP-[^{3}H]-GlcNAc. Control values were 4,500 ± 500 cpm (n = 8) for transport, 1,600 ± 200 cpm (n = 8) for glycosylation, 2,500 ± 400 cpm (n = 8) for uptake, 6,400–16,700 cpm for integrity, and 7,100 ± 500 cpm (n = 2) for sedimentation. (*B*) Reaction mixtures contained 0.25 μCi UDP-[^{3}H]-Gal. Control values were 900 ± 150 cpm (n = 8) for glycosylation and 3,500 ± 500 cpm (n = 8) for uptake. (*C*) Reaction mixtures contained 0.25 μCi of CMP-[^{3}H]-sialic acid. Control values were 1,300 ± 300 cpm (n = 8) for glycosylation and 9,300 ± 1,100 cpm (n = 8) for uptake.

VSV-g protein glycosylation after it has been delivered to the acceptor compartment. To test this possibility, transport reactions were incubated in the absence of UDP-[^{3}H]-GlcNAc for 45 min to accumulate VSV-g protein in the acceptor compartment. Inhibitory concentrations of the peptides were added and the incubation continued for an additional 15 min. The membranes were then re-isolated and incubated in glycosylation buffer containing UDP-[^{3}H]-GlcNAc in the absence of peptides (20).

When the membranes are not exposed to peptides at the end of the transport incubation, the level of glycosylation observed in the second stage (Fig. 4, *control*) is equivalent to the amount of glycosylation measured when UDP-[^{3}H]-GlcNAc is added at the beginning of the transport reaction (dashed line; 20). In contrast, when membranes are treated with either MAS or NEM after transport is complete, subsequent glycosylation is inhibited. Identical results were obtained with ARFp13 (data not shown). These data also demonstrate that the inhibition of glycosylation is irreversible, since the free peptides were removed prior to the glycosylation incubation. Neither peptide was found to inhibit the activity of Gal transferase or GlcNAc transferase in soluble enzyme assays, indicating that inhibition was not due to a direct inhibitory effect of the peptides on glycosyl transferases (data not shown).

The Peptides Inhibit Uptake of Sugar Nucleotide Precursors by Golgi Membranes

To further investigate the mechanism by which these peptides inhibit glycosylation, VSV-infected wild type Golgi were used to measure uptake of nucleotide sugars and the incorporation of radiolabeled sugars into VSV-g protein already residing in the various Golgi biosynthetic compartments (47). The membranes were incubated under the same conditions that reconstitute transport, but transport was prevented by inactivation of endogenous NSF (5). Fig. 5 *A* shows that concentrations of MAS, ARFp13, NEM, and SDS that optimally inhibit transport have a similarly inhibitory effect on the glycosylation of VSV-g protein and uptake of UDP-[^{3}H]-GlcNAc, suggesting that inhibition of glycosylation is due to the absence of luminal UDP-[^{3}H]-GlcNAc in the Golgi membranes. Fig. 5 (*B* and *C*) show that these inhibitory effects on nucleotide sugar uptake and glycosylation are not restricted to compartments containing the GlcNAc/UMP translocase. There is also significant inhibition of uptake and glycosylation when UDP-[^{3}H]-galactose and CMP-[^{3}H]-sialic acid are used as substrates, although the extent of inhibition is generally not as severe.

Inhibition of nucleotide-sugar uptake could occur if these compounds directly inhibit the nucleotide-sugar translocators, or if they permeabilize the membranes. To distinguish between these possibilities, the integrity of the membranes after incubation with the peptides, as assessed by their ability to maintain a performed gradient of UDP-[^{3}H]-GlcNAc, was determined. As shown in Fig. 5 *A*, ARFpl3 and SDS appear to directly inhibit uptake, since the integrity of the membranes is only partially compromised. In contrast, inhibition of uptake by MAS and NEM correlates with near complete loss of membrane integrity. This loss of integrity was not, however, due to a significant breakdown of Golgi structure per se. 90% or more of Golgi proteins pre-labeled with [^{3}H]-GlcNAc during a 60-min incubation without inhibitors still sedimented with the membranes after a second incubation that included the inhibitors (Fig. 5 *A*). It therefore seems likely that inhibition of nucleotide sugar uptake is due to a sub-lytic detergent-like effect of these peptides, and not to activation of a trimeric G protein.

Inhibition of Transport Is Insensitive to Agents That Modify G Protein Activity

The IC_{50}'s for inhibition of the overall transport reaction by MAS and ARFpl3 are consistently lower than the IC_{50}'s for inhibition of glycosylation alone (Table II *A*). This increased sensitivity of the transport assay could be due to a specific effect of the peptides on GTP-binding proteins, which might be masked by the non-specific effects on protein glycosylation occurring at slightly higher peptide concentrations. If this is true, then treatments that prevent the peptides from modulating GTP-binding protein activity would be expected to decrease the sensitivity of the transport assay to the peptides. Since these treatments would not affect the non-specific inhibition of glycosylation, the IC_{50} for transport should increase to the same level observed for inhibition of glycosylation alone. To test this possibility, several treatments that have previously been shown to block the effects of MAS in other systems were examined.

The fungal metabolite, brefeldin A (BFA) can prevent either MAS-induced (26) or GTPγS/ARF-induced binding of β-COP to Golgi membranes (17). In addition, BFA overcomes the inhibition of in vitro Golgi transport caused by GTPγS and ARF (38). Table II *B* shows that BFA is completely ineffective at increasing the IC_{50} for MAS or ARFpl3 in the transport assay, even though inhibition by GTPγS was blocked under the same conditions. The effects of MAS can also be abrogated by pre-treating the cells with pertussis toxin (26, 29), suggesting that the target of MAS is one of the pertussis toxin-sensitive trimeric G proteins, G_i or G_o. As shown in Table II *C*, Golgi membranes prepared from pertussis toxin-treated cells are just as susceptible as untreated membranes to inhibition of transport by these peptides. Lastly, since GTP is required for activation of GTP-binding proteins, we tested whether the effect of the peptides on transport would be altered by including GTP in the assay. Table II *D* shows that 50 μM GTP was without effect on the IC_{50} for transport. We conclude that inhibition of transport by these peptides is unrelated to specific effects on the function of GTP-binding proteins, and is most likely due to a general disruptive effect of the peptides on membrane function.

Table II. Inhibition of In Vitro Transport by the Peptides Is Insensitive to Agents that Modulate GTP-binding Protein Activity

	MAS	ARFp13
	IC_{50} (μM)	
(*A*) Time of peptide addition		
(*a*) low total protein		
before transport	0.8	18
before glycosylation	1.9	27
(*b*) high total protein		
before transport	2.0	35
before glycoslyation	2.8	45
(*B*) Addition of BFA		
0 μM	2.2	36
200 μM	2.0	34
(*C*) Pertussis toxin treatment		
mock-treated membranes	1.3	29
treated membranes	1.3	30
(*D*) Addition of GTP		
0 μM	1.4	27
50 μM	1.3	27

The IC_{50} was determined from titration curves as described in Table 1. (*A*) Peptide was addded either prior to initiating the transport reaction, as in Figure 1, or after transport was completed but before glycosylation, as in Figure 3. (*a*) The cytosol and membrane protein concentrations were 0.29 and 0.12 mg/ml, respectively. (*b*) The cytosol and membrane protein concentrations were 0.56 and 0.22 mg/ml, respectively. (*B*) Each titration contained the indicated concentration of BFA with 0.58 mg/ml cytosol and 0.13 mg/ml membranes. Control samples demonstrated that BFA was effective at preventing inhibition of transport by GTPγS under these conditions. (*C*) Donor and acceptor membranes were prepared from pertussis toxin-treated cells, as described in Materials and Methods. Approximately 80% of the reactive G subunits were ribosylated, and the specific transport activities of mock-treated and -untreated membranes were indentical (see Materials and Methods for details). Assays contained 0.35 mg/ml cytosolic and 0.07 mg/ml membrane protein. (*E*) Assays contained the indicated concentrations of GTP with 0.30 mg/ml cytosol and 0.2 mg/ml membrane protein. The variation in control IC_{50} values is due to the different cytosol and membrane protein concentrations in each experiment.

The Peptides Have Complex Effects on Golgi Ultrastructure

Our biochemical analysis demonstrates that the effects of MAS and ARFpl3 on in vitro transport are indistinguishable. Nevertheless, previous studies have documented that these peptides have the exact opposite effects on binding of β-COP to Golgi membranes (24, 26). To further investigate this paradox, we used a new technique for obtaining high resolution, three-dimensional images of immobilized Golgi after in vitro incubation to examine the effect of the peptides on Golgi morphology (53). For these experiments, the concentrations of cytosol and peptides were adjusted to compensate for the low concentration of immobilized membranes in the in vitro incubations (see Materials and Methods for details).

The morphology of immobilized Golgi membranes incubated with the non-inhibitory peptides, MAS17 and ARFp28, was indistinguishable from that of control membranes (Fig. 6 *A*) incubated without peptides, and the density of coated buds and vesicles was also the same (Fig. 7 *A*). In contrast, Golgi cisternae with typical morphology decreased in abundance or were altogether absent after a 10-min incubation at 37°C with either MAS or ARFpl3 (Fig. 7 *A*). Instead, cisternae with clusters of uncoated bud-like structures at the periphery (Fig. 6 *C*), and regions of irregular vesicles, tubules, and membrane discs suggestive of shattered cister-

nae (Fig. 6 *D*) were seen. At higher concentrations of cytosol and peptides, cisterna-like structures with long tubular loops were also observed. In some cases, the tubular loops exhibited patches of a dense, punctate coat and coated buds (Fig. 6 *E*). In other instances the tubules were smooth surfaced (Fig. 6 *F*). All of these aberrant forms were observed with both peptides, with the exception that tubular cisternae with a dense punctate coating (Fig. 6 *E*) were more frequently observed with MAS than ARFp13. These effects were only occasionally observed after treatment with SDS. However, SDS-treated membranes had a lower density of coated buds (Fig. 7 *A*) and frequently appeared swollen and distorted, as though they were in the process of pulling away from the substrate (cisternae in top right corner, Fig. 6 *B*). Similarly distended cisternae were also occasionally observed after incubation with low concentrations of peptides. With the possible exception of the shattering of membranes, the disruption of morphology induced by the peptides is not a direct consequence of immobilization of the membranes. The same abnormalities were observed when membranes were incubated with MAS in suspension, and then attached to the coverslips (data not shown).

Quantitative analysis revealed a coordinate decrease in the density of coated buds and vesicles and in the fraction of cisternae exhibiting normal morphology with increasing concentration of MAS or ARFp13 (Fig. 7, *B* and *C*). This decrease paralleled the inhibition of in vitro Golgi transport measured in reactions containing the same concentrations of membrane and cytosolic protein. In addition, the density of Golgi and other contaminating membranes on the coverslips also decreased. Approximately 9–14 profiles of Golgi stacks or individual cisternae were observed per 55 × 55 μm grid space in control incubations. In samples incubated with the highest concentrations of peptides, this value fell to one or less profile per grid space with a commensurate decrease in non-Golgi membranes, suggesting that membranes had detached during the incubation. These results suggest that both inhibition of in vitro Golgi transport and inhibition of coated vesicle formation are due to membrane damage induced by the peptides, and not to a specific effect on Golgi vesicle dynamics, in agreement with the biochemical evidence.

Since these Golgi membrane preparations contain contaminating plasma membrane fragments, it is possible that the membrane disruption observed could be due to activation of plasma membrane–associated trimeric G proteins with subsequent activation of soluble phospholipases. We therefore determined whether inactivation of G_i and G_o, the presumed targets of MAS, by pertussis toxin–catalyzed ADP-ribosylation prevented the morphological changes induced by incubation with MAS (Table III *A*). Pertussis toxin treatment had no effect on the transport activity of Golgi membranes (see Materials and Methods for details) or on the IC_{50} for inhibition of transport by either MAS or ARFp13 (Table II). This treatment did, however, result in a 1.4-fold increase in Golgi-coated bud and vesicle density after a 10 min in vitro transport incubation (Table III *A*; also compare Figs. 6 *A* and 8 *A*). Although small, this increase was statistically significant when compared with mock-treated membranes in the same experiment ($P < 0.05$), and with all of the control membranes analyzed in this study (four preparations, $P < 0.01$). The ability of MAS to disrupt the morphology of pertussis toxin–treated membranes was similar to that observed with mock-treated membranes. Pertussis toxin–treated cisternae with disrupted morphology exhibited the same gross abnormalities as mock-treated membranes, but had a significantly higher density of coated buds (Fig. 8 *B*, Table III *A*). The ability of MAS to alter the morphology of pertussis toxin–treated membranes confirms our conclusion that these morphological changes are the result of the detergent-like properties of MAS.

In the experiments described above, the membranes were incubated in vitro for only 10 min. Since a significant population of cisternae with apparently normal morphology was observed after short incubations at peptide concentrations at or below the IC_{50} (Fig. 7, *B* and *C*), it was of interest to know whether these populations would maintain normal morphological characteristics during the longer incubations required to measure transport in the in vitro assay. We have previously shown that a 10-min in vitro incubation is sufficient to establish a steady state of vesicle production and consumption on immobilized Golgi (53). After prolonged incubation, the coated bud and vesicle density increases 1.3–1.5-fold (*control*, Table III *B*), but the size of cisternae decreases commensurately (53), suggesting that vesicles are continuously released but do not efficiently transfer in this system. When immobilized membranes were incubated with either MAS or ARFp13, coated bud and vesicle densities increased 2.5–3-fold between 10 and 45 min of incubation, to nearly twice the level observed with untreated membranes (Table III *B*). This increase occurred without a commensurate decrease in the size of cisternae, and did not result in the accumulation of fully formed vesicles that failed to detach. Of the coated structures that could be clearly identified (at least 60% of the total), ~85% were coated buds in all three 45 min samples. There was also a notable decrease in the fraction of cisternae exhibiting abnormal morphology after 45 min of incubation, suggesting that these cisternae may represent a subpopulation of the original membranes. These data demonstrate that, after incubation with MAS or ARFp13, even cisternae with apparently normal morphology exhibit abnormal coated bud and vesicle dynamics.

Discussion

We have biochemically and morphologically characterized the mechanism of action of two amphipathic peptides, MAS and ARFp13, on in vitro Golgi transport. These peptides were previously thought to specifically interfere with the function of two distinct GTP-binding proteins that regulate Golgi-coated vesicle dynamics, and have been shown to have opposing effects on Golgi vesicle coat protein binding (24, 26). Our detailed analysis reveals that both peptides inhibit in vitro Golgi transport by inducing membrane damage, and not by specifically interfering in GTP-binding protein function. We further demonstrate that, at concentrations below those that completely disrupt cisternal architecture and inhibit in vitro transport, both MAS and ARFp13 have subtle effects on Golgi-coated bud and vesicle dynamics. While the damaging effects of the peptides are not reversed by pertussis toxin–treatment of the membranes, this treatment alone also has a subtle effect on coated vesicle dynamics. These results raise important issues concerning both the interpretation of

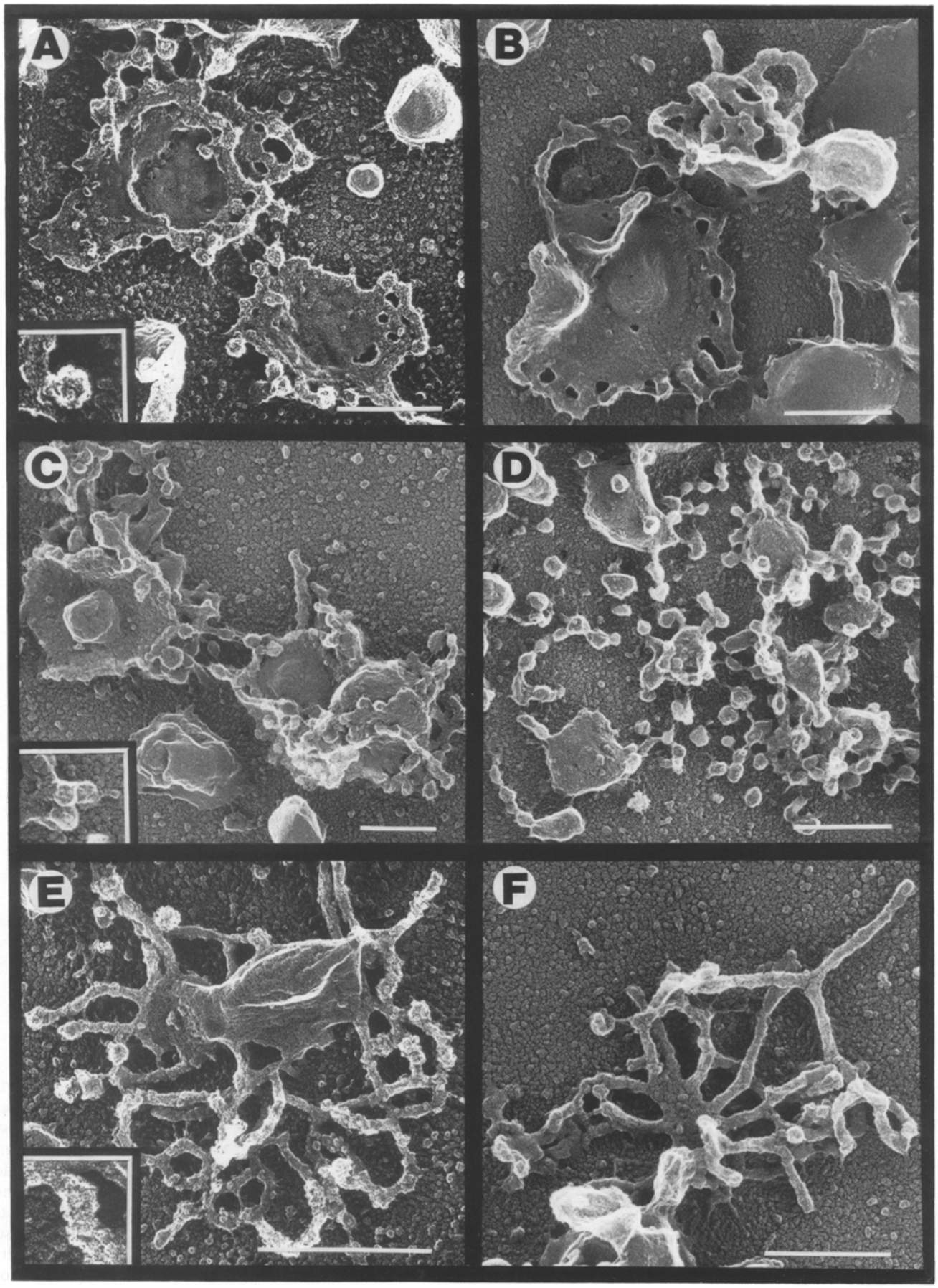
A
B
C
D
E
F

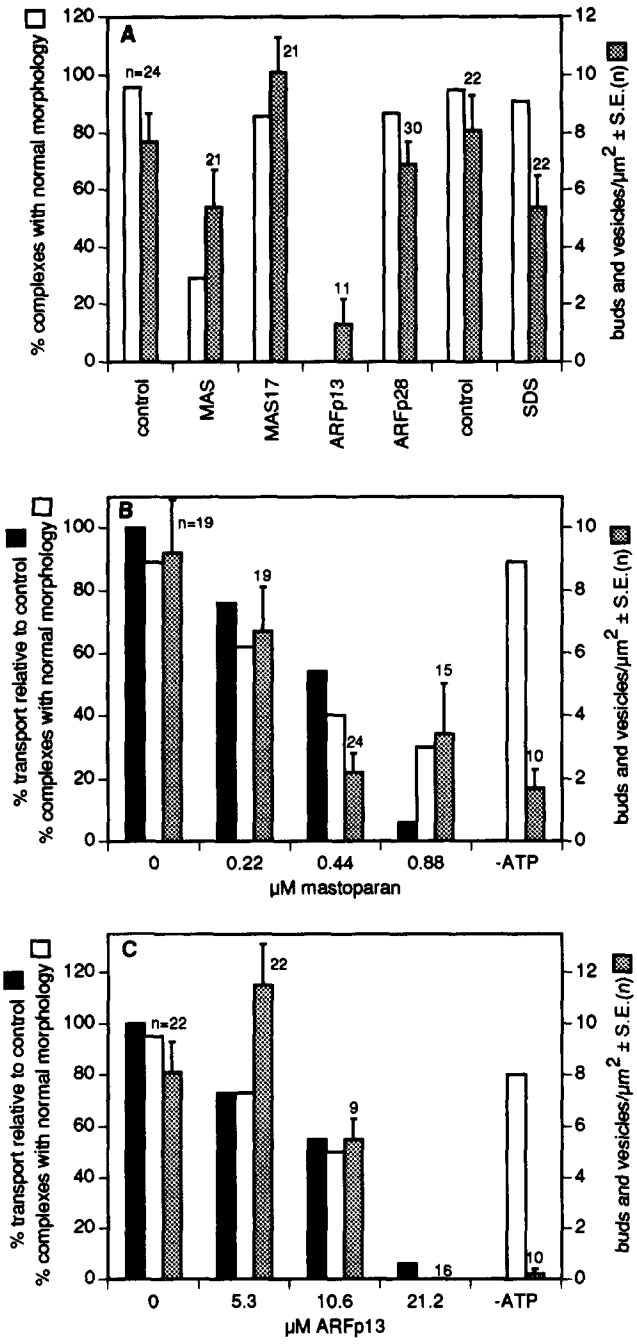

Figure 7. Disruption of cisternal structure and reduced coated bud and vesicle density is specific for MAS and ARFp13, and correlates with inhibition of transport. Immobilized Golgi membranes were incubated for 10 min in vitro, and processed for electron microscopy as described in Materials and Methods. Randomized negatives were scored for the density of coated buds and vesicles (*stippled bars*), and for abnormal morphological characteristics such as swelling, clusters of uncoated buds, long tubules and shattering, as shown in Fig. 5 (C–F). Data are reported as the fraction of cisternae exhibiting normal morphology (*open bars*). (*A*) Immobilized membranes were incubated for 10 minutes without inhibitors (*control*) or with 1.8 μM MAS, 2.0 μM MAS17, 42 μM ARFp13, 45 μM ARFp28, or 50 μM SDS in a transport mixture containing 2 mg/ml cytosol. The IC_{50} for inhibition of in vitro transport under similar conditions was approximately 1.0 μM for MAS and 20 μM for ARFp13. (*B* and *C*) Membranes were incubated for 10 min with a transport reaction mixture containing 1 mg/ml cytosol and inhibitors as indicated. ATP was omitted from one control reaction (*−ATP*) to determine the nominal levels of normal cisternae and bud density under conditions that do not support budding. In vitro transport (*black bars*) was measured in 100 μl reactions containing 0.01 mg/ml membrane protein and the same cytosol at 1 mg/ml. The results are expressed as percent of transport relative to the control incubation without peptide (900 ± 100 cpm, $n = 4$). The increase in bud and vesicle density on membranes incubated with 5.3 μM ARFp13 is statistically significant (Wilcoxon rank sum test, $P < 0.05$).

previous studies that used these peptides and the use of peptides in general as specific reagents for analyzing protein function in complex in vitro systems.

The Primary Mechanism of Inhibition of In Vitro Golgi Transport

Our biochemical and morphological data strongly support the conclusion that inhibition of transport and glycosylation by these peptides is due to disruption of the membrane. Both peptides form amphipathic helices that can partition into membranes (21, 24) and other have reported that high concentrations of MAS can damage membranes (21, 29). To our knowledge, however, this is the first report to specifically document these effects in biological membranes, and to demonstrate generalized membrane disfunction at peptide concentrations below those necessary to completely permeabilize membranes.

Sublytic concentrations of ARFp13 and SDS exhibit distinct concentration-dependent effects on membrane function. Transport was most sensitive to inhibition, while slightly higher concentrations inhibited facilitated membrane transport, and even higher concentrations were needed to completely permeabilize the membranes (Fig. 5 *A*, Table II). A similar effect was observed with MAS (Table II), although inhibition of facilitated transport and permeabilization of the membranes could not be resolved. Surprisingly, the alkylating agent, NEM, completely permeabilized the membranes after a short incubation at 37°C. This effect is specific for the oxidized form of NEM, since reduced NEM does not inhibit transport (2). Although the mechanism of permeabilization is unclear, this finding raises the possibility that inhibition of various membrane functions by NEM could be due to an effect on membrane lipids rather than on proteins, as commonly assumed.

The effects of the peptides on membrane function are paralleled by an increase in the fraction of cisternae exhibiting

Figure 6. Inhibitory concentrations of MAS and ARFp13 drastically alter Golgi cisternal architecture. Golgi membranes were immobilized on coverslips, incubated with in vitro transport reaction mixtures for 10 min at 37°C, and replicas of the quick frozen, deep-etched membranes prepared for electron microscopy, as described in Materials and Methods. Transport incubations included: (*A*) no inhibitors; (*B*) 50 μM SDS; (*C*) 0.44 μM MAS; (*D*) 10.6 μM ARFp13; (*E*) 1.8 μM MAS; and (*F*) 42 μM ARFp13. The cytosol concentration was 1 mg/ml in A-D and 2 mg/ml in E and F. Insets were magnified 2.5-fold to reveal the ultrastructure of (*A*) the punctate coat on Golgi buds, (*C*) lack of a punctate coat on buds, and (*D*) punctate coat on the surface of a tubule. Bars, 0.3 μm.

Table III. Coated Bud and Vesicle Dynamics Are Modified by MAS, ARFp13, and Pertussis Toxin Treatment of Membranes

Incubation conditions	Buds and vesicles $\mu m^2 \pm$ S.E. (n)	Percent normal complexes	Buds and vesicles $\mu m^2 \pm$ S.E. (n)	Percent normal complexes
(*A*) Comparison of untreated and pertussis toxin-treated membranes				
	Mock treated		Pertussis toxin treated	
control	9.7 ± 0.3 (22)	82	13.5 ± 0.3 (20)	80
0.44 μM MAS	11.7 ± 0.9 (20)	50	7.2 ± 0.3 (21)	43
0.88 μM MAS	2.5 ± 0.5 (12)	0	7.6 ± 0.8 (14)	14
(*B*) Comparison of short and long incubations				
	10-min incubation		45-min incubation	
control	7.7 ± 1.0 (24)	96	10.1 ± 1.7 (18)	100
0.44 μM MAS	7.6 ± 0.9 (19)	74	18.3 ± 3.0 (17)	89
10.6 μM ARFp13	5.5 ± 0.8 (9)	50	18.8 ± 2.2 (17)	94

Sample preparation and analysis were as described for Fig. 7. (*A*) Membranes prepared from either mock or pertussis toxin-treated cells, as shown in Table II and described in Materials and Methods, were incubated with 1 mg/ml cytosol and the indicated concentrations of MAS for 10 min. The IC_{50} for inhibition of transport under similar conditions was 0.4 μM MAS. The difference in bud and vesicle density between mock and pertussis toxin-treated control membranes is statistically significant (Wilcoxon rank sum test, $P < 0.05$). The majority of pertussis toxin-treated Golgi membranes identified after incubation with 0.88 μM MAS were budding cisternal fragments that were, on the average, half the size of normal cisternae. (*B*) Membranes were incubated in a transport reaction mixture with 2 mg/ml cytosol, as described in Fig. 7 *A*. Half of the reactions were terminated after 10 min and the remainder incubated for 45 min. The elevated bud and vesicle densities observed after 45 min of incubation with the peptides are statistically significant (Wilcoxon rank sum test, $P < 0.02$ for MAS and $P < 0.01$ for ARFp13).

morphological changes such as distortion of cisternal shape, elaboration of bud-like protrusions or long tubules, and fragmentation of membranes (Fig. 6). A similar tubularization of cisternae is observed after membranes are incubated with ATP in the absence of cytosol (53). We have suggested that these long tubules form on cisternae by rearrangement of the peripheral tubular networks in response to the loss of a stabilizing protein coat that is distinct from vesicle coats (53). It is therefore of interest that peptide-induced disruption of the membrane also resulted in tubular rearrangements (Fig. 6, *E* and *F*), even though some tubules exhibited a punctate surface coating similar to that found on vesicles (Fig. 6 *E*). It is also of interest that the peptides caused an increase in the fraction of cisternae with abnormal morphology as their concentrations were increased, rather than causing a gradation of effects on the entire population. Since partition coefficients are sensitive to lipid composition, and the lipid composition, especially the cholesterol content, varies across the Golgi stack (8), it is possible that cisternae on one side of the stack are more resistant to the damaging effects of the peptides. This is consistent with the observation that uptake of UDP-gal and CMP-sialic acid, presumably in the

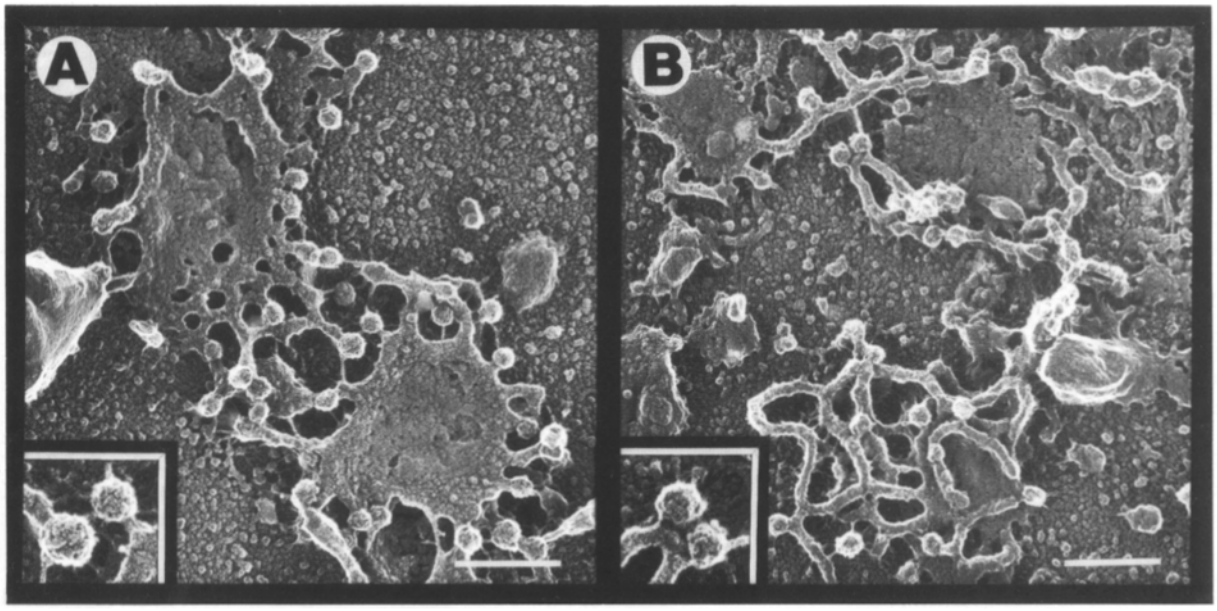

Figure 8. Membranes from pertussis toxin-treated cells exhibit higher densities of coated vesicles but are not resistant to MAS-induced disruption of morphology. Membranes prepared from pertussis toxin-treated cells, as described in Materials and Methods, were incubated in vitro for 10 min, and then prepared for electron microscopy as described in Fig. 5. (*A*) No inhibitor; (*B*) 0.44 μM MAS. Insets are magnified 2.5-fold to reveal the punctate coat on the buds. Bars, 0.3 μm.

trans-most cisternae, is less sensitive to inhibition by the peptides (Fig. 5, *B* and *C*).

The fragmentation of membranes induced by the peptides (Fig. 6 *D*) seems to contradict the finding that membranes incubated with the peptides in suspension are readily sedimented (Fig. 5 *A*). Since the immobilized membranes are covalently attached to the coverslips, this shattering may occur when the membranes are unable to accommodate membrane expansion induced by intercalation of the peptides. The sedimentation velocity of membranes treated with MAS is slightly greater than that of untreated membranes (Weidman, P., unpublished results), suggesting that the peptides do induce membrane swelling. Lastly, although the biochemical effects of SDS closely paralleled those of the peptides, its effects on morphology were minimal (Fig. 6 *B*). This may reflect differences between the shape or volume occupied by SDS and the peptides in the lipid bilayer, and/or the ability of these compounds to transfer to the inner leaflet of the bilayer, as suggested by Sheetz and Singer in the bilayer couple hypothesis (42).

ARFpl3 Is Not a Specific Inhibitor of ARF Activity

Our data clearly show that inhibition of vesicle formation by ARFpl3 is due to disruption of membrane structure, and not to competition with ARF as originally proposed (24). This difference in interpretation is not due to any subtle difference between our system and that of Kahn et al., since they also found that Golgi cisternae were rarely seen after incubation with ARFpl3 (24). Such a non-specific mechanism of inhibition explains the lack of competition between ARF and ARFpl3, and the inhibition of in vitro Golgi transport by ARFpl3, even though ARF is not required for transport (47). This same mechanism may underlie the inhibition of transport observed in other in vitro systems (3, 28, 34), since similar concentrations of ARFpl3 were required, and competition between ARF and the ARF peptides for inhibition was not demonstrated.

Limitations of Mastoparan as a Tool for Analyzing Trimeric G Protein Function in Biological Systems

Several studies have provided evidence that MAS increases Golgi coat protein binding and alters vesicle dynamics by modulating trimeric G protein activity. In permeabilized cells, 10 μM MAS stimulates β-COP binding to Golgi membranes, and this effect is diminished either by pertussis toxin-treatment or by brefeldin A (26). In addition, 25 μM MAS caused a 10-fold increase in the amount of β-COP bound to isolated Golgi membranes (26). p200 is BFA-sensitive protein localized on *trans*-Golgi vesicles that accumulate after treatment with GTPγS or AlF (36). Its binding to rat liver Golgi membranes in vitro is stimulated more than sevenfold by 100 μM MAS, and this stimulation is also diminished by pertussis toxin treatment (9). Despite the implication that activation of trimeric G proteins stimulates Golgi vesicle formation, inhibition rather than stimulation of transport is observed in vivo (45). An alternative perspective has come from functional studies of vesicle release from the TGN (29). At much lower concentrations (1 μM), MAS7 partially suppresses the release of both constitutive and regulated vesicles from the TGN of PC12 cells in vitro. Pertussis toxin–catalyzed ADP ribosylation of $G_{\alpha i/o}$ subunits stimulates vesicle release almost twofold and renders it insensitive to MAS. Vesicle release is also enhanced when $G_{\alpha s}$ subunits are activated by cholera toxin–catalyzed ADP ribosylation. It has been proposed that these paradoxical findings could be reconciled if coated bud production is stimulated by activation of $G_{\alpha s}$ and fission of coated buds to produce coated vesicles is suppressed by activation of $G_{\alpha i/o}$ (32). One of our objectives was to directly test this hypothesis using a combination of functional assays and high resolution ultrastructural analyses.

It is clear from our functional analysis that the ability of MAS to inhibit in vitro Golgi transport is independent of pertussis toxin-sensitive pathways. In retrospect, this is not surprising, since we have recently demonstrated that transport in this system is independent of Golgi-coated vesicles (47). The effects of MAS reported in the studies described above are partly (9, 26) or fully (29) reversed by pertussis toxin treatment, and similar effects are obtained with AlF_4, suggesting that increased coat protein binding and changes in vesicle dynamics are associated with activation of trimeric G proteins. Nevertheless, our ultrastructural analysis suggests that MAS has the potential to introduce artifacts that complicate the elucidation of the mechanisms involved. For example, incubation of membranes with high concentrations of MAS and cytosol resulted in the elaboration of cisternal tubules that were encrusted with punctate material resembling the coats found on Golgi vesicles (Fig. 6 *E*). Assuming this punctate coat corresponds to vesicle coat proteins, this would represent a substantial increase in the level of coat protein binding to Golgi membranes. Since this effect was seldom observed with ARFpl3, this accumulation might be the consequence of trimeric G protein activation. Alternatively, it has recently been shown that coatomers will bind to the di-lysine retention motif of ER membrane proteins (14). A high density of lysine residues exposed on the cytoplasmic surface of Golgi, as would occur when MAS partitions into membranes, might thus serve as novel binding sites for coatomers. This possibility is of particular concern given that the massive increase in coat protein binding observed in in vitro binding assays occurred at extremely high levels of MAS, and was only partially inhibited by pertussis toxin treatment (9, 26).

The accumulation of coated buds that occurred on a subset of cisternae after prolonged incubation of membranes with MAS (Table III *B*) provides an example of the difficulty in interpreting more subtle effects of MAS. This increase seemed to arise by a decrease in the rate of vesicle formation from buds, as opposed to a stimulation of budding, since it was not apparent early in the incubation, and the majority of coated structures that accumulated were buds, not vesicles. Although the increase was relatively small (1.8–1.9-fold), it is consistent with the modest effect of MAS on release of vesicles from the TGN (~30% inhibition, 29), but not with the substantial increase in coat protein binding observed in other studies. If this increase is due to activation of trimeric G proteins, these findings would support the proposed model for dual regulation of Golgi vesicle dynamics described above. However, it is also possible that slowing of vesicle fission is a general effect of low concentrations of membrane perturbants, since ARFpl3 also induced a similar increase in bud and vesicle density.

A final observation bearing on the function of trimeric G proteins in Golgi vesicle dynamics is the 1.4-fold increase in the density of Golgi-coated buds and vesicles seen on pertussis toxin-treated membrane after a short transport incubation (Table III *A*). This increase, although small, was significant when compared to all of the control membranes examined in this study, and was seen even on cisternal fragments produced during incubations with MAS. This increase might be due to a stimulation of coated bud formation, since it was apparent very early in the incubation, and its magnitude is similar to the stimulation of TGN vesicle release observed after pertussis toxin treatment (approximately a 1.6–1.7-fold increase; 29).

The subtle effects of MAS and pertussis toxin treatment on Golgi vesicle dynamics are thus consistent with the effects of these same treatments on vesicle release from the TGN (29), yet are inconclusive with regard to the mechanisms involved. The pronounced membrane perturbing effects of these peptides suggest that alternative methods of approach will be needed to unravel the complexity of trimeric G protein involvement in membrane transport.

Implications for Studies Using These and Other Peptide Reagents

These studies demonstrate that the criteria for peptide specificity accepted in the past are inadequate to rule out nonspecific effects in such complex in vitro systems. In particular, using peptides that have been shown to be inactive with purified proteins as indicators of specificity can be quite misleading, as demonstrated by the data in Fig. 2. Comparing the behavior of peptides with similar tendency to form amphipathic helices in the presence of lipid is also not sufficient, since the propensity of ARFp13 and the non-inhibitory peptide, MAS17, to form α helices in the presence of lipids is nearly identical (22, 24), yet MAS17 had no effect on in vitro transport at concentrations up to 50 μM (Weidman, P., unpublished observation). Lack of membrane permeabilization over the effective concentration range would also appear to be insufficient, since ARFp13 did not significantly permeabilize membranes at the concentrations needed to effect inhibition of transport (Fig. 5 *A*). Moreover, our data suggest that the partition coefficient of peptides may vary with the lipid composition of the membrane, such that acceptable concentrations for one intracellular membrane could be disruptive for another. A further complication is the apparent inactivation of peptides by cytosol, which makes it difficult to know the actual peptide concentration, and gives the erroneous impression that there is specific competition between the peptide and a cytosolic factor.

These considerations and the observation that not all peptides with an affinity for membranes form amphipathic α helices (25), raise the legitimate concern that more stringent controls are needed when any peptide reagent is used in such biological systems. One obvious criteria is that inhibition by a peptide should be preventable or reversible. For example, inhibition should be overcome by competition with the protein from which the peptide was derived, or by adding excess target protein. Alternatively, inhibition should be reversed upon removal of the peptide. Secondly, the peptide should not affect facilitated membrane transport in the membrane of interest, even at concentrations twofold higher than the effective range for inhibition of the process under study. Thirdly, morphological changed such as organelle swelling, distortion, fragmentation, or a decrease in abundance of membranes with recognizable morphology should be viewed with suspicion. Lastly, there may be independent criteria that can be applied. For example, it is clear that BFA and pertussis toxin treatment had no effect on the inhibition of transport by MAS or ARFp13.

In summary, we do not believe that our findings negate the utility of peptides as specific reagents for probing protein function, but they do emphasize the need for a stricter approach in assessing the specificity of peptide action in biological systems, especially when membrane-dependent processes are involved.

The authors thank Drs. Paul Melançon, Steve Scholnick, Maureen Linder, and Steve Fleisler for their helpful comments during the preparation of this manuscript. We also gratefully acknowledge Dr. Maureen Linder for performing the in vitro ADP-ribosylation assays, Drs. Marissa Colombo and Philip Stahl for providing MAS7 and MAS17, and Drs. Julie Donaldson and Richard Klausner for providing ARFp13 and ARFp28. We are especially indebted to Dr. John Heuser and Ms. Robyn Roth for preparing the replicas of freeze-etched membranes, and to Dr. Heuser for generously giving us access to his electron microscopes.

This research was funded by American Cancer Society grants BE-87 and BE-73473 to P. Weidman.

Received for publication 26 July 1994 and in revised form 6 September 1994.

References

1. Balch, W. E., W. G. Dunphy, W. A. Braell, and J. E. Rothman. 1984. Reconstitution of the transport of protein between successive compartments of the Golgi measured by the coupled incorporation of N-acetylglucosamine. *Cell.* 39:405–416.
2. Balch, W. E., B. S. Glick, and J. E. Rothman. 1984. Sequential intermediates in the pathway of intercompartmental transport in a cell-free system. *Cell.* 39:525–536.
3. Balch, W. E., R. A. Kahn, and R. Schwaninger. 1992. ADP-ribosylation factor (ARF) is required for vesicular trafficking between the endoplasmic reticulum (ER) and the cis Golgi compartment. *J. Biol. Chem.* 267:13053–13061.
4. Barr, F. A., A. Leyte, and W. B. Huttner. 1992. Trimeric G proteins and vesicle formation. *Trends Cell Biol.* 2:91–93.
5. Block, M. R., B. S. Glick, C. A. Wilcox, R. T. Wieland, and J. E. Rothman. 1994. Purification of an N-ethylmaleimide-sensitive protein catalyzing vesicular transport. *Proc. Natl. Acad. Sci. USA.* 85:7852–7856.
6. Bokoch, G. M., T. Katada, J. K. Northup, M. Ui, and A. G. Gilman. 1984. Purification and properties of the inhibitory guanine nucleotide-binding component of adenylate cyclase. *J. Biol. Chem.* 259:3560–3567.
7. Bomsel, M., and K. Mostov. 1992. Role of heterotrimeric G proteins in membrane traffic. *Mol. Biol. Cell.* 3:1317–1328.
8. Bretscher, M. S., and S. Munro. 1994. Cholesterol and the Golgi apparatus. *Science (Wash. DC).* 261:1280–1281.
9. Bruno de Almeida, J., J. Doherty, D. A. Ausiello, and J. L. Stow. 1993. Binding of the cytosolic p200 protein to Golgi membranes is regulated by heterotrimeric G proteins. *J. Cell Sci.* 106:1239–1248.
10. Carter, L. L., T. E. Redelmeier, L. A. Woollenweber, and S. L. Schmid. 1993. Multiple GTP-binding proteins participate in clathrin-coated vesicle-mediated endocytosis. *J. Cell Biol.* 120:37–45.
11. Clary, D. O., and J. E. Rothman. 1990. Purification of three related peripheral membrane proteins needed for vesicular transport. *J. Biol. Chem.* 265:10109–10117.
12. Colombo, M. I., S. Gonzalo, P. Weidman, and P. Stahl. 1991. Characterization of trypsin-sensitive factor(s) required for endosome-endosome fusion. *J. Biol. Chem.* 266:23438–23445.
13. Colombo, M. I., L. S. Mayorga, P. J. Casey, and P. D. Stahl. 1992. Evidence of a role for heterotrimeric GTP-binding proteins in endosome fusion. *Science (Wash. DC).* 255:1695–1697.
14. Cosson, P., and F. Letourner. 1994. Coatomer interaction with di-lysine endoplasmic reticulum retention motifs. *Science (Wash. DC).* 263: 1629–1631.
15. Dascher, C., and W. E. Balch. 1994. Dominant inhibitory mutants of ARF1 block endoplasmic reticulum to Golgi transport and trigger disassembly of the Golgi apparatus. *J. Biol. Chem.* 269:1437–1448.
16. Davidson, J. S., A. Eales, R. W. Roeske, and R. P. Millar. 1993. Inhibition

of pituitary hormone exocytosis by a synthetic peptide related to the rab effector domain. *FEBS (Fed. Eur. Biochem. Soc.) Lett.* 326:219–221.
17. Donaldson, J. G., R. A. Kahn, J. Lippincott-Schwartz, and R. D. Klausner. 1991. Binding of ARF and β-COP to Golgi membranes: possible regulation by a trimeric G-protein. *Science (Wash. DC).* 254:850–853.
18. Dunphy, W. G., and J. E. Rothman. 1983. Compartmentation of Asparagine-linked oligosaccharide processing in the Golgi apparatus. *J. Cell Biol.* 97:270–275.
19. Heuser, J., and L. Evans. 1980. Three-dimensional visualization of coated vesicle formation in fibroblasts. *J. Cell Biol.* 84:560–583.
20. Hiebsch, R. R., and B. W. Wattenberg. 1992. Vesicle fusion in protein transport through the Golgi in vitro does not involve long-lived prefusion intermediates. A reassessment of the kinetics of transport as measured by glycosylation. *Biochemistry.* 31:6111–6118.
21. Higashijima, T., S. Uzu, T. Nakajima, and E. M. Ross. 1988. Mastoparan, a peptide toxin from wasp venom, mimics receptors by activating GTP-binding regulatory proteins (G proteins). *J. Biol. Chem.* 263:6491–6494.
22. Higashijima, T., J. Burnier, and E. M. Ross. 1990. Regulation of G_i and G_o by mastoparan, related amphiphilic peptides and hydrophobic amines. *J. Biol. Chem.* 265:14176–14186.
23. Hirs, C. H. W. 1967. Detection of peptides by chemical methods. *Methods Enzym.* 11:325–329.
24. Kahn, R. A., P. Randazzo, T. Serafini, O. Weiss, C. Rulka, J. Clark, M. Amherdt, P. Roller, L. Orci, and J. E. Rothman. 1992. The amino terminus of ADP-ribosylation factor (ARF) is a critical determinant of ARF activities and is a potent and specific inhibitor of protein transport. *J. Biol. Chem.* 267:13039–13046.
25. Kaiser, E. T., and F. J. Kezdy. 1987. Peptides with affinity for membranes. *Ann. Rev. Biophys. Biophys. Chem.* 16:561–581.
26. Ktistakis, N. T., M. E. Linder, and M. G. Roth. 1992. Action of brefeldin A blocked by activation of a pertussis-toxin-sensitive G protein. *Nature (Lond.).* 356:344–346.
27. Lang, L., and S. Kornfeld. 1984. A simplified procedure for synthesizing large quantities of highly purified uridine-[^{32}P]diphospho-N-acetylglucosamine. *Anal. Biochem.* 140:263–269.
28. Lenhard, J. M., R. A. Kahn, and P. D. Stahl. 1992. Evidence for ATP-ribosylation factor (ARF) as a regulator of in vitro endosome-endosome fusion. *J. Biol. Chem.* 267:13047–13052.
29. Leyte, A., F. A. Barr, R. H. Kehlenbach, and W. B. Huttner. 1992. Multiple trimeric G-proteins on the trans-Golgi network exert stimulatory and inhibitory effects on secretory vesicle formation. *EMBO (Eur. Mol. Biol. Organ.) J.* 11:4795–4804.
30. Li, G., R. Regazzi, W. E. Balch, and C. B. Wollheim. 1993. Stimulation of insulin release from permeabilized HIT-T15 cells by a synthetic peptide corresponding to the effector domain of the small GTP-binding protein rab3. *FEBS (Fed. Eur. Biochem. Soc.) Lett.* 327:145–149.
31. MacLean, C. M., G. J. Law, and J. M. Edwardson. 1993. Stimulation of exocytotic membrane fusion by modified peptides of the rab3 effector domain: re-evaluation of the role of rab3 in regulated exocytosis. *Biochem. J.* 294:325–328.
32. Melançon, P. 1993. G whizz. *Curr. Biol.* 3:230–233.
33. Melançon, P., B. S. Glick, V. Malhotra, P. J. Weidman, T. Serafini, M. L. Gleason, L. Orci, and J. E. Rothman. 1987. Involvement of GTP-binding "G" proteins in transport through the Golgi stack. *Cell.* 51:1053–1062.
34. Morgan, A., and R. D. Burgoyne. 1993. A synthetic peptide of the N-terminus of ADP-ribosylation factor (ARF) inhibits regulated exocytosis in adrenal chromaffin cells. *FEBS (Fed. Eur. Biochem. Soc.) Lett.* 329: 121–124.
35. Moss, J., and M. Vaughan. 1993. ADP-ribosylation factors, 20,000 M_r guanine nucleotide-binding protein activators of cholera toxin and components of intracellular vesicular transport systems. *Cell. Signalling.* 4:367–379.
36. Narula, N., I. McMorrow, G. Plopper, J. Doherty, K. S. Matlin, B. Burke, and J. L. Stow. 1992. Identification of a 200-kD, brefeldin-sensitive protein on Golgi membranes. *J. Cell Biol.* 117:27–38.
37. Novick, P., and P. Brennwald. 1993. Friends and family: the role of the Rab GTPases in vesicular traffic. *Cell.* 75:597–601.
38. Orci, L., M. Tagaya, M. Amherdt, A. Perrelet, J. G. Donaldson, J. Lippincott-Schwartz, R. D. Klausner, and J. E. Rothman. 1991. Brefeldin A, a drug that blocks secretion, prevents the assembly of non-clathrin-coated buds on Golgi cisternae. *Cell.* 64:1183–1195.
39. Plutner, H., R. Schwaninger, S. Pind, and W. E. Balch. 1990. Synthetic peptides of the Rab effector domain inhibit vesicular transport through the secretory pathway. *EMBO (Eur. Mol. Biol. Organ.) J.* 9:2375–2383.
40. Richmond, J., and P. G. Haydon. 1993. Rab effector domain peptides stimulate the release of neurotransmitter from cell cultured synapses. *FEBS (Fed. Eur. Biochem. Soc.) Lett.* 326:124–130.
41. Robinson, M. S., and T. E. Kreis. 1992. Recruitment of coat proteins onto Golgi membranes in intact and permeabilized cells: effects of brefeldin A and G protein activators. *Cell.* 69:129–138.
42. Sheetz, M. P., and S. J. Singer. 1974. Biological membranes as bilayer couples. A molecular mechanism of drug-erythrocyte interactions. *Proc. Natl. Acad. Sci. USA.* 71:4457–4461.
43. Smith, P. K., R. I. Krohn, G. T. Hermanson, A. K. Mallia, F. H. Gartner, M. D. Provenzano, E. K. Fujimoto, N. M. Goeke, B. J. Olson, and D. C. Klenk. 1985. Measurement of protein using bicinchoninic acid. *Anal. Biochem.* 150:76–85.
44. Stanley, P., V. Caillibot, and L. Siminovitch. 1975. Selection and characterization of eight phenotypically distinct lines of lectin-resistant Chinese Hamster Ovary cells. *Cell.* 6:121–128.
45. Stow, J. L., J. Bruno de Almeida, N. Narula, E. J. Holtzman, L. Ercolani, and D. A. Ausiello. 1991. A heterotrimeric G protein, G_{i-3}, on Golgi membranes regulates the secretion of a heparan sulfate proteoglycan in LLC-PK, epithelial cells. *J. Cell Biol.* 114:1113–1124.
46. Taylor, T. C., and P. Melançon. 1992. Two distinct members of the ADP-ribosylation factor family of GTP-binding proteins regulate cell-free intra-Golgi transport. *Cell.* 70:69–79.
47. Taylor, T. C., M. Kanstein, P. Weidman, and P. Melançon. 1994. Cytosolic ARFs are required for vesicle formation but not for cell-free intra-Golgi transport: evidence for coated vesicle-independent transport. *Mol. Biol. Cell.* 5:237–252.
48. Teal, S. B., V. W. Hsu, P. J. Peters, R. D. Klausner, and J. G. Donaldson. 1994. An activating mutation in ARF1 stabilizes coatomer binding to Golgi membranes. *J. Biol. Chem.* 269:3135–3138.
49. Tisdale, E. J., J. R. Bourne, R. Khosravi-Far, C. J. Der, and W. E. Balch. 1994. GTP-binding mutants of Rab1 and Rab2 are potent inhibitors of vesicular transport from the endoplasmic reticulum to the Golgi complex. *J. Cell Biol.* 119:749–761.
50. Waldman, B. C., and G. Rudnick. 1990. UDP-GlcNAc Transport across the Golgi membrane: electroneutral exchange for dianionic UMP. *Biochemistry.* 29:44–52.
51. Wattenberg, B. W., W. E. Balch, and J. E. Rothman. 1986. A novel prefusion complex formed during protein transport between Golgi cisternae in a cell-free system. *J. Biol. Chem.* 261:2202–2207.
52. Wattenberg, B. W., T. J. Raub, R. R. Hiebsch, and P. J. Weidman. 1992. The activity of Golgi transport vesicles depends on the presence of the N-ethylmaleimide Sensitive Factor (NSF) and a Soluble NSF Attachment Protein (SNAP) during vesicle formation. *J. Cell Biol.* 118:1321–1332.
53. Weidman, P., R. Roth, and J. Heuser. 1993. Golgi membrane dynamics imaged by freeze-etch electron microscopy: views of different membrane coatings involved in tubulation versus vesiculation. *Cell.* 75:123–133.
54. Zhang, C.-J., A. G. Rosenwald, M. C. Willingham, S. Skuntz, J. Clark, and R. A. Kahn. 1994. Expression of a dominant allele of human ARF1 inhibits membrane traffic in vivo. *J. Cell Biol.* 124:289–300.